Contents lists available at ScienceDirect

Journal of Photochemistry & Photobiology, A: Chemistry

Fluorescent water-stable quantum dots possessing benzimidazole for the recognition of bisulfate in edible materials, soap, and medicine

Gitanjali Jindal , Navneet Kaur [*]

Department of Chemistry, Panjab University, Chandigarh 160014, India

A B S T R A C T

Fluorescent and water-stable ZnO quantum dots have been synthesized from its organic precursor appended with benzimidazole for the detection of bisulfate anion. The characterization of the quantum dots has been done using high-resolution transmission electron microscopy (HRTEM), powder X-ray diffraction (PXRD), UV–visible (UV–vis), and Fluorescence (FL) spectroscopy. The fluorescent properties of quantum dots made them useful for the sensing of bisulfate ions in different real-life samples such as edible materials, medicines, and soap solutions. They have been successfully applied for the detection of bisulfate in these samples with good recovery. Their fluorescence responses towards bisulfate ion enabled them to be used as efficient fluorescent sensors in the water.

1. Introduction

In recent times, different techniques have been developed to recognize and sense biologically and environmentally important species and this has turn out to be a considerable aim in the area of chemical sensors [1]. Despite the fact that anions are identified to play foremost tasks in our everyday life and extensively in chemical and biological processes, they are becoming the target of research that includes their sensing, in the last decade. As a consequence, anionic species can either act as harmful pollutants or they can be essential to sustain growth in the environment [2–4].

The need of hour is the requirement of sensors for the anions as a result of severe troubles posed by them such as excess fluoride consumption causes fluorosis [5], excess of cyanide results in hypoxia, and exposure to a higher concentration of sulfide leads to various physiological [6] and biochemical effects. Amongst all these anions, bisulfate (HSO_4^-) acquires a definite place. At alkaline pH, bisulfate (HSO_4^-) ions dissociate to produce noxious sulfate (SO_4^{2-}), which can cause skin and eyes irritation and also lead to respiratory paralysis [7–9]. It plays a very significant role in a number of chemical processes [10], for example, sulfate ions help with binding protein in transport systems [11] as an essential bio-molecular group. However, diversely, it is lethal to the environment due to its presence in fertilizers, pollutants, nuclear wastes [12], and industrial raw materials. Conventionally, humans eat up bisulfate naturally through a daily diet. There are cruciferous plant foods such as cabbage, broccoli, mustard seeds (both black and white

varieties), and carrot from the umbellifer family which comprises endogenous bisulfate that is generated by the enzymatic reaction of the sinigrin substrate [13–15] and myrosinase enzyme. Bisulfate consumption also takes place by means of drugs. For instance, quinine bisulfate, clopidogrel bisulfate, neomycin bisulfate, etc., are available in the market as bisulfate salts to improve their water solubility [16]. Therefore, to exonerate these complications, this is utterly essential to recognize and extort bisulfate ions from various achievable resources.

In spite of the essential roles played by anions in biological processes, only a small number of systems for anion sensing have been stated in the literature. However, the basic limitation of all these systems is their deficiency in recognizing the considered necessary anions in aqueous media [17], caused by solubility crisis. As a result, the development of such sensors which have the capability to work in aqueous solutions is considerable and extremely desirable.

Recently, quantum dots (QDs) which are one of the special classes of semiconductors with sizes ranging from 1 to 10 nm are gaining much attention from scientists [18–21]. They display strong luminescent properties and have emerged as a group of highly fluorescent sensing materials [22–29]. The size of a quantum dot varies inversely with the band gap energy levels which modify the frequency of light and affects the colour emitted. The small-sized dots produce higher energy light which has a blue colour, while the large-sized dots generate low energy red light. Also, the size of the material can be controlled by varying temperatures and the time duration of the synthesis reaction [30]. Amidst a number of detection systems, fluorescent sensing techniques

are more useful because with these sensors, no reference is required and the analyte can be reused. Moreover, the instrumentation procedures have simplicity and facilitate rapid response time [31–34].

Among various types of materials used for the synthesis of quantum dots, ZnO has attained a great deal of consideration in different fields and has been utilized in photocatalysts, sensors, piezoelectric devices, solar cells, transparent electrodes, laser diodes, [35–39] and so on. This metal oxide is able to form a large number of excitons which allow it to display fluorescence at room temperature [35]. In comparison to the bulk material, it demonstrates advanced optical properties as soon as they are constrained to the size of quantum dots [40]. Owing to its environment-friendly nature and economic semiconducting characteristics, it can substitute a variety of other semiconductor nanomaterials such as CdSe or CdTe that have characteristics of showing large luminescence [41].

In the present work, water-stable fluorescent quantum dots, based on ZnO, *1-QDs,* have been synthesized from an organic molecule **1** possessing benzimidazole for the sensitive detection of hydrogen sulfate anions. The sensing properties of molecule **1** and the corresponding quantum dots have been discussed in the $CH_3CN:H_2O$ (2:1, v/v) (pH = 7, HEPES buffer) solution. Also, various daily utilized products have been tested for the presence of bisulfate ion with which the quantum dots can be easily applied for recognition of HSO_4^- ion in real life.

2. Experimental

2.1. Materials and methods

Benzil, 2-hydroxy-4-methoxybenzaldehyde, zinc acetate, sodium hydroxide, perchlorate salts of metal ions, and tetrabutylammonium salts of various anions were purchased from Aldrich. The mustard seeds, carrots, soap, and medicines were purchased from the local market. Acetonitrile (CH_3CN) used was of HPLC grade. Melting points were evaluated using capillary and were uncorrected. Proton (^1H) and Carbon (^{13}C) NMR spectra were recorded on BRUKER AVANCE 500 and 125 MHz instruments using tetramethylsilane as an internal standard. Various metal ions such as Al^{3+}, Na^+, K^+, Mg^{2+}, Mn^{2+}, Fe^{2+}, Co^{2+}, Ni^{2+}, Cu^{2+}, Zn^{2+}, Hg^{2+}, and Cd^{2+} were added as their perchlorate salts and anions such as F^-, Cl^-, Br^-, I^-, OH^-, AcO^-, HSO_4^-, $H_2PO_4^-$, SO_4^- and CN^- were added as their tetrabutylammonium salts for UV–vis and fluorescence experiments. Aliquots of all the ions under investigation were then injected into the sample solution through a rubber septum in the cap. The solutions were permitted to obtain stability after each addition and were then scanned.

2.2. General procedure for HRTEM, XRD, UV–vis, and fluorescence experiments

UV–vis and fluorescence titrations were performed on 20 μM and 1 μM concentrations, respectively, of **1** in $CH_3CN:H_2O$ (2:1, v/v) (pH = 7, HEPES buffer) solution. And for the *1-QDs,* these experiments were carried out on 2 mg/100 mL solution in 2:1 (v/v) aqueous acetonitrile (pH 7.0 HEPES buffer). All the UV–vis experiments were conducted on JASCO UV-750 spectrometer; while fluorescence spectra were recorded using HITACHI-7000 spectrophotometer operated with 220–240 V Xenon lamp and quartz cell of 1 cm width and height of 3.5 cm. The excitation was carried out at 350 nm for sensor **1** with 5 nm excitation as well as emission slit widths in the fluorometer. Stock solution of the sensor **1** (1×10^{-2} M) was prepared in DMSO and was diluted with aqueous CH_3CN (v/v 2:1; pH = 7) solution for further spectroscopic experiments. All absorption profiles were saved as ACS type II files and then processed in Excel (TM) to generate all graphs shown. High-Resolution Transmission Electron Microscopic (HRTEM, Hitachi H7500 electron microscope) analysis (100 kV) was executed to measure the size and morphology of the quantum dots, *1-QDs.* XRD analysis was carried out to evaluate the crystalline size and phases of the as-

synthesized quantum dots utilizing a scan rate of 2 deg min^{-1} in XRD powder diffractometer (Panalytical X'Pert Pro) with Cu-Kα radiation.

2.3. Synthesis of 2-(4,5-Diphenyl-1H-imidazol-2-yl)-5-methoxy-phenol (1)

The chemosensor **1** has been synthesized by reacting benzil and 2-hydroxy-4-methoxybenzaldehyde in glacial acetic acid (Scheme 1). The reactants, benzil (4.75 mmol, 1 gm) and ammonium acetate (137 mmol, 10.55 gm) were added in 10 mL of hot glacial acetic acid. To this reaction mixture, a solution of 2-hydroxy-4-methoxybenzaldehyde (4.75 mmol, 0.722 gm) in 10 mL of glacial acetic acid was added. The mixture was heated at 90 °C for 5 hrs and the progress of reaction was monitored by TLC. After the reaction was completed, the mixture was transferred to 200 mL of water. Then, the solution was neutralized with ammonium hydroxide to pH = 7 and cooled to room temperature. The precipitates were filtered to yield crude product and washed with a large amount of water. Recrystallization of crude product from mixture of methanol and chloroform resulted in formation of pure product **(1)**. White-grey soild; 92% yield; m.p. (°C) 216; FT-IR (neat, ν cm^{-1}): 3230 (O–H$_{str.}$), 3056 (Ar–H$_{str.}$), 1506 (Ar-C=C$_{str.}$), 1620 (–C=N$_{str.}$), 1292 (–C–N$_{str.}$); ^1H NMR (500 MHz, DMSO-d_6, ppm) **:** 13.10 (brs, 1H, –OH), 12.82 (brs, 1H, –NH), 7.95 (d, 1H, Ar-H), 7.53–7.41 (m, 6H, Ar-H), 7.45 (t, 1H, Ar-H), 7.34 (t, 2H, Ar-H, J_1 = 7.7 Hz and J_2 = 7.4 Hz), 7.26 (t, 1H, Ar-H, J = 7.3 Hz), 6.57–6.53 (m, 2H, Ar-H), 3.78 (–OCH$_3$); ^{13}C NMR (125 MHz, DMSO-d_6, ppm): 160.8, 158.3, 146.1, 133.6, 130.2, 128.6, 128.3, 126.8, 126.4, 125.8, 106.1, 105.8, 101.3, 55.1; LCMS : m/z (relative abundance (%), assignment) = 343.15 [100, (M + 1)$^+$]. ^1H NMR, ^{13}C NMR and LCMS spectra of **1** have been shown in Figs. S1–S3.

2.4. Synthesis of quantum dots (1-QDs)

A facile synthesis route to synthesize *1-QDs* was adopted. Firstly, 2 mmol (0.438gm) of Zn(OAc)$_2$·2H$_2$O was dissolved in 50 mL ethanol using ultrasonication and then 3 mmol (0.906gm) of **1** was added to it. Further, 0.5 mmol (0.02gm) of NaOH was dissolved in 5 mL of ethanol and it was added dropwise to Zn(OAc)$_2$ solution under vigorous stirring at room temperature. After 2hrs, the white–grey suspension was obtained which was centrifuged at 8000 rpm to separate the precipitates. The precipitates were re-dispersed in ethanol and centrifuged again. This process was repeated twice to remove unreacted material in the solution and finally *1-QDs* were obtained in pure form. XRD, FTIR and HRTEM techniques were used to measure the size and morphology of synthesized quantum dots (Figs. S4–S5 and Fig. 1).

2.5. Characterization of quantum dots (1-QDs)

2.5.1. XRD studies of 1-QDs

To evaluate the atomic and molecular structure of the synthesized quantum dots, XRD studies were carried out. Fig. S4 has displayed the XRD patterns of a dried form of *1-QDs* and respective information about the crystalline/amorphous nature of QDs. The peak obtained at 22.17° indicated the crystalline nature of formed QDs. The crystallite size was
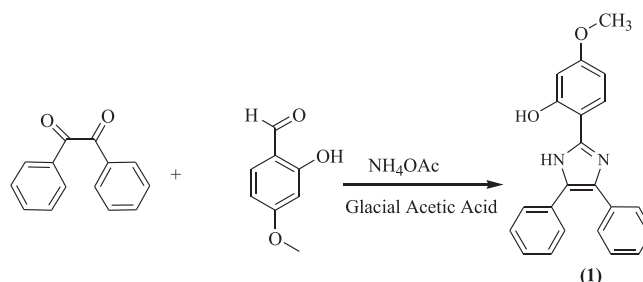
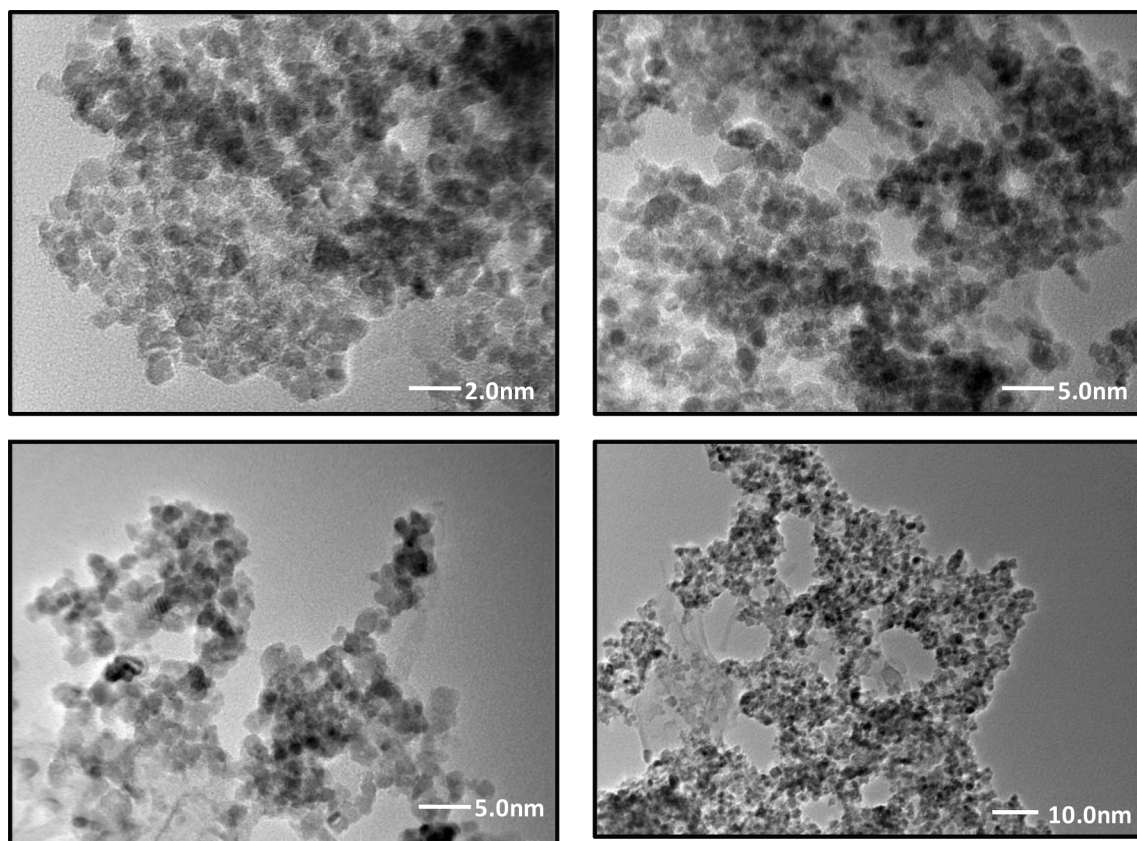**Scheme 1.** Synthetic route for the formation of sensor **1**.

Fig. 1. HRTEM images of **1**-QDs.

determined to be 4.006 Å by using Bragg's equation corresponding to this angle (22.17°):

$$d = \lambda/2 sin\Theta,$$

where λ is the wavelength of the X-ray beam (0.154 Å), d is the distance between the adjacent sheets or layers, θis the diffraction angle. The major diffraction peak for quantum dots was observed at 2Θ = 22.17°, 31.97°, 33.19°, 34.51° and 36.06°. There was observed no additional peak related to impurities which imply that ZnO-QDs obtained are highly pure.

2.5.2. FT-IR analysis of 1-QDs

FT-IR studies were performed for the surface characterization of *1-QDs*. Fig. S5a–b shows the comparison of FT-IR spectrum of **1** with that of *1-QDs*. Peaks obtained for *1-QDs* (Fig. S5b) at 3466 cm^{-1} correspond to N–H stretching vibrations, peak centered at 2033 cm^{-1} corresponds to aromatic C–H vibrations, while the peak at 485 cm^{-1} corresponds to Zn–O bond. The two finely separated peaks at 1636 and 1617 cm^{-1} clearly indicated the interaction of ZnO with compound **1**. Also, the peak at 1506 cm^{-1} in spectra of **1** (Fig. S5a) was found susceptible to binding of **1** with ZnO and was shifted to 1488 cm^{-1} as can be seen in spectra (Fig. S5b) of *1-QDs* [42–45].

2.5.3. HRTEM (particle size) studies of 1-QDs

The topological and size distribution studies were done by using high-resolution transmission electron microscopic (HRTEM) analysis. The obtained HRTEM images of the quantum dots (*1-QDs*) have shown spherical particles with a diameter of 2–10 nm (Fig. 1). These images depict that the particles obtained are a little polydisperse in nature.

3. Results and discussion

3.1. Fluorescence emission spectral response of 1

To assess the sensing ability of sensor **1** towards a variety of metal ions including Na$^+$, K$^+$, Mg^{2+}, Al^{3+}, Mn^{2+}, Fe^{2+}, Co^{2+}, Ni^{2+}, Cu^{2+}, Zn^{2+}, Hg^{2+}and Cd^{2+} and anions such as F$^-$, Cl$^-$, Br$^-$, I$^-$, OH$^-$, AcO$^-$, HSO$_4^-$, H$_2$PO$_4^-$ and SO$_4^-$, initially the UV–vis spectral responses of **1** (20 μM) in 2:1 (v/v) aqueous CH$_3$CN (pH = 7, HEPES buffer) were noted. The absorption spectrum of sensor **1** exhibits two peaks at 285 and 322 nm. Upon the incorporation of 100 equiv. of above-referred metal ions and anions to CH$_3$CN:H$_2$O (2:1, v/v) (pH = 7, HEPES buffer) of sensor **1**, negligible changes were detected in the absorption spectrum (Fig. S6) of **1**. Although, there were observed absorbance peaks of higher intensity below 300 nm which were attributable to Cu^{2+} and Hg^{2+} ions' own absorbance. Hence, any definite variations studied with Cu^{2+} and Hg^{2+} cannot be recognized.

On the other hand, sensor **1** exhibited a strong emission at 425 nm (λ$_{ex}$ = 350 nm). Among various anions and metal ions investigated, only addition of Hg^{2+}, Cu^{2+}, and Al^{3+} ions to the solution of **1** (1 μM; CH$_3$CN: H$_2$O (2:1, v/v) (pH = 7, HEPES buffer) affected its fluorescence; (as shown in Fig. 2a) wherein Hg^{2+} and Cu^{2+} quenched and Al^{3+} ions enhanced the fluorescence intensity. These fluorescence changes were accompanied by color changes (Fig. 2b) from light fluorescent blue to light yellow for Hg^{2+}, yellowish-green for Cu^{2+}, and dark blue color in case of Al^{3+} ions when irradiated with light (λ$_{ex}$ = 350 nm). Importantly, all tested anions exhibited no fluorescence response for **1** under the same spectroscopic conditions (Fig. S7).

The binding behavior of **1** with M^{n+} (Hg^{2+}, Cu^{2+}, and Al^{3+}) was further investigated through fluorescence titrations by adding standard solutions of detected ions to 1 μM solution of sensor molecule **1**. Upon gradual addition of Cu^{2+}, the fluorescence intensity started quenching steadily with negligible spectral shift (Fig. 3a); while Hg^{2+} addition
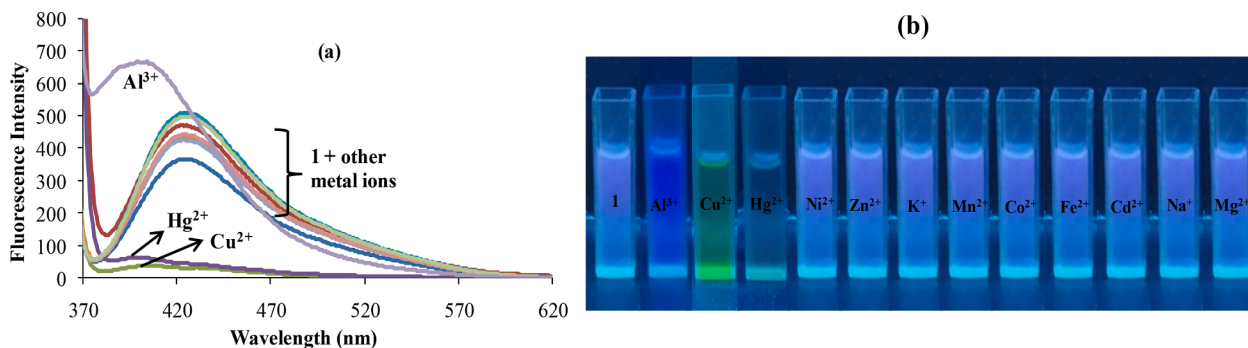
Fig. 2. (a) Fluorescence spectral response of **1** in CH₃CN:H₂O (2:1, v/v) (pH = 7, HEPES buffer) upon addition of 100 equiv. of different metal ions; (b) Fluorescence colorimetric changes in the presence of various metal ions.
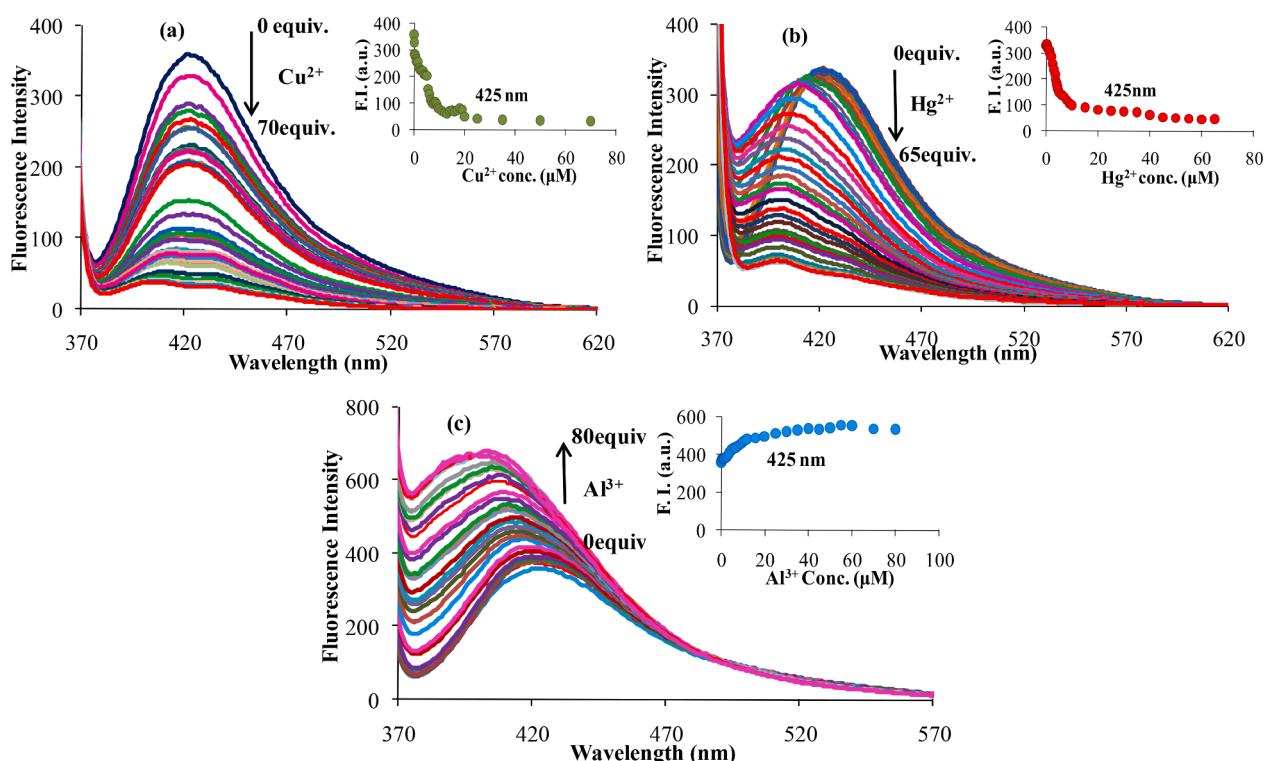
Fig. 3. Fluorescence titration studies (λ_{ex} = 350 nm) of **1** (1 μM) in CH₃CN:H₂O (2:1, v/v) (pH = 7, HEPES buffer) in the presence of different concentrations of sensed metal ions: (a) Cu²⁺, (b) Hg²⁺ and (c) Al³⁺ cations. Inset: Plot of fluorescence intensity at 425 nm versus the concentration of added, (a) Cu²⁺, (b) Hg²⁺ and (c) Al³⁺ cations.

caused a slight blue shift in the spectrum (Fig. 3b). On the other hand, with the continuous incorporation of Al³⁺ ion to the solution of **1**, there was noticed a significant blue shift from 425 to 395 nm (Fig. 3c).

The binding constant between sensor **1** and Cu²⁺ was calculated to be 2.43×10^5 M⁻¹ on the basis of fluorescence titrations using the Benesi-Hildebrand equation given below [46];

$$1/F - F = 1/F_{max} - F_o + 1/[F_{max} - F_o]K[C]$$

here, F_o, F, and F_{max} is the fluorescence of free **1**, measured with Cu²⁺ and measured with an excess amount of Cu²⁺ at 425 nm. K is the association constant and [C] is the concentration of Cu²⁺ ions added. The detection limit was calculated using equation LOD = 3σ/ρ [47] and was estimated to be 8.95 μM. The binding constant of Hg²⁺ and Al³⁺ were determined to be 2.72×10^5 and 1.42×10^5 M⁻¹, respectively. From the changes in Al³⁺ and Hg²⁺ dependent fluorescence intensity, the detection limit was estimated to be 1.5 and 1.97 μM, respectively.

3.2. Fluorescence studies of **1**-QDs

The fluorescent properties of **1-QDs** were evaluated with a concentration of 2 mg in 100 mL in CH₃CN:H₂O (2:1, v/v) (pH = 7, HEPES buffer) solution. The **1-QDs** exhibited a broad band at 423 nm on excitation at 350 nm (Fig. 4a). Among various anions and metal ions investigated (Fig. S8), the addition of Hg²⁺, and Cu²⁺ ions to solution of **1-QDs** in CH₃CN:H₂O (2:1, v/v) (pH = 7, HEPES buffer) quenched its fluorescence intensity peak at 423 nm; whereas HSO₄⁻ enhanced the fluorescence intensity to a remarkable extent under similar conditions (Fig. 4b).

The binding between **1-QDs** and sensed ions (Hg²⁺, Cu²⁺, and HSO₄⁻) were further scrutinized via fluorescence titration experiments by incorporating standard solutions of corresponding ions to the solution of **1-QDs** (2 mg/100 mL).

Upon gradual addition of Cu²⁺, the fluorescence intensity at 423 nm experienced steady quenching with the insignificant spectral shift as
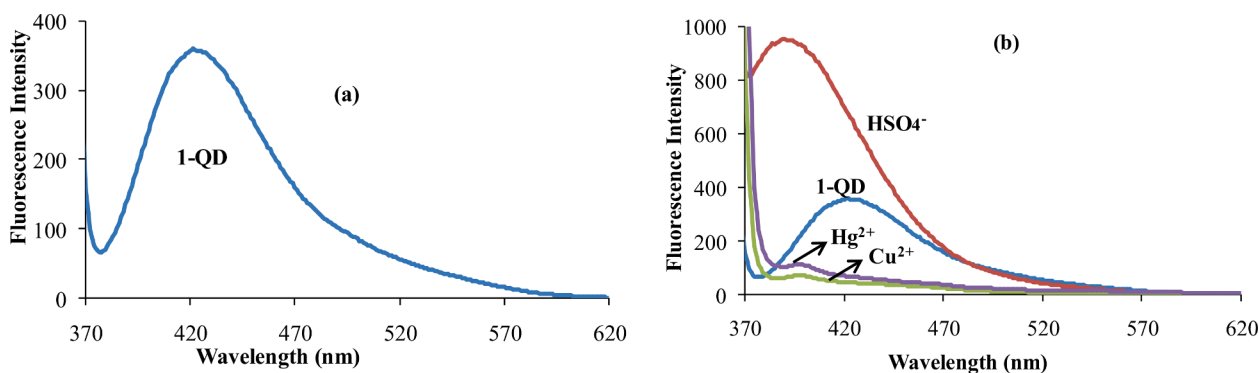
Fig. 4. (a) Fluorescence spectrum of *1-QDs* in CH$_3$CN:H$_2$O (2:1, v/v) (pH = 7, HEPES buffer); (b) fluorescence changes in the presence of sensed (Cu^{2+}, Hg^{2+}, and HSO$_4^-$) ions excited at 350 nm.

shown in Fig. 5a. In case of Hg^{2+} ion, there was observed a small shift in the spectrum towards the shorter wavelength with progressive addition of Hg^{2+} ion (Fig. 5b). Also, with the continuous incorporation of HSO$_4^-$ ion to the solution of *1-QDs*, there was noticed a remarkable blue shift from 423 to 397 nm (Fig. 5c). The association coefficient between *1-QDs* and HSO$_4^-$ was estimated to be 7.98 × 10^4 M^{-1} on the basis of fluorescence titrations through the Benesi-Hildebrand equation given below [46];

$$1/F - F_o = 1/F_{max} - F_o + 1/[F_{max} - F_o]K[C]$$

here, F$_o$ is the fluorescence of free *1-QDs*, F is measured with HSO$_4^-$, and F$_{max}$ is fluorescence measured at 423 nm with an excess amount of HSO$_4^-$. K is the association constant and [C] is the concentration of HSO$_4^-$ ions added. The limit of detection was calculated using equation LOD = 3σ/ρ [47] and was estimated to be 3.17 nM. The association constant of Cu^{2+} and Hg^{2+} were determined to be 9.74 × 10^4 and 5.2 ×

10^4 M^{-1} correspondingly. From the changes in Cu^{2+} or Hg^{2+} dependent fluorescence intensity, the detection limit was found as 2.91 and 8.35 μM, respectively. Furthermore, the long-lasting nature of the synthesized quantum dots, *1-QDs*, was tested by examining the fluorescence behavior and HRTEM after 10 and 20 days (Fig. S9a–b). They unveiled that there was negligible change in the morphology, structure, and sensitivity when stored in the appropriate state for more than 20 days.

3.3. Real life applications

To examine the applicability of *1-QDs* in real-life, it was tested for the determination of HSO$_4^-$ ions in soap, medicine, and edible materials (Fig. 6). For this examination, about 1gm of mustard seeds, 5gm of chopped broccoli, and 5gm of grated carrot were taken, mixed with 5–10 mL of water and then grinded to extract their juice. The obtained extract was used for the qualitative investigation of HSO$_4^-$ ion [48]. The
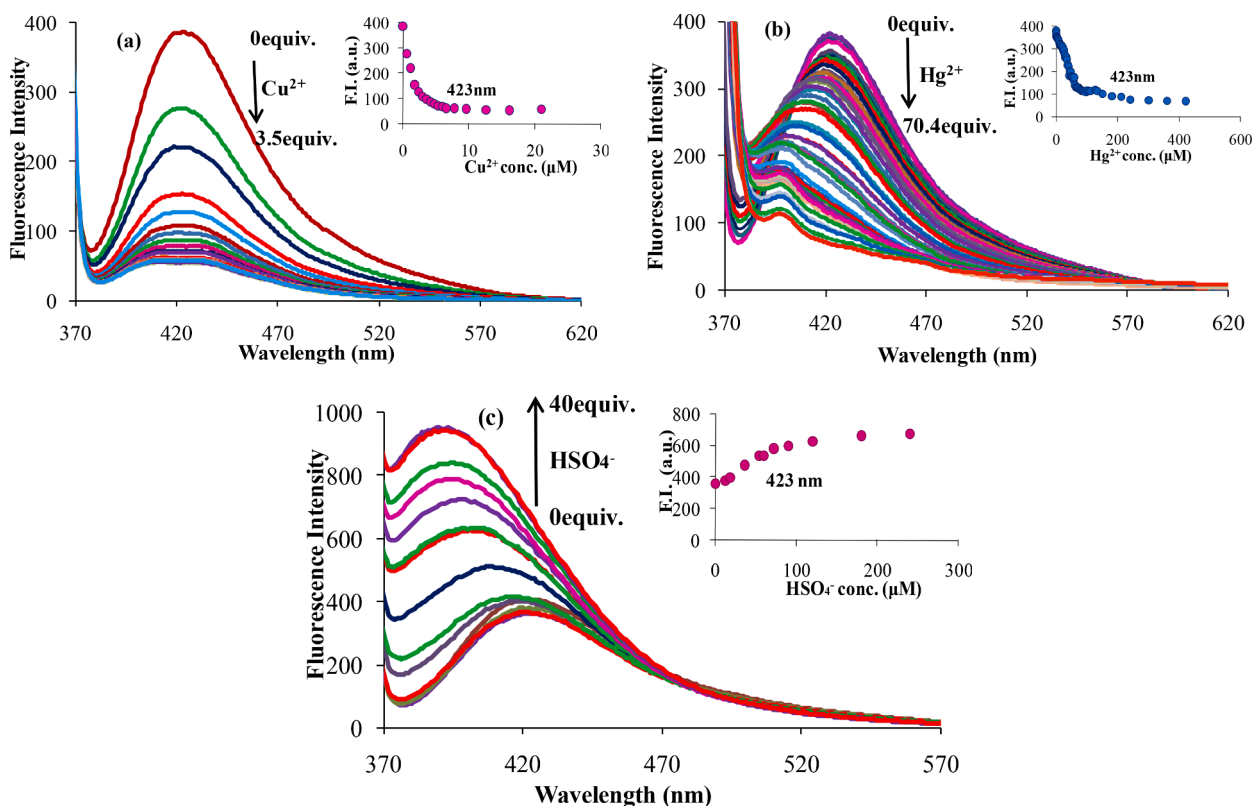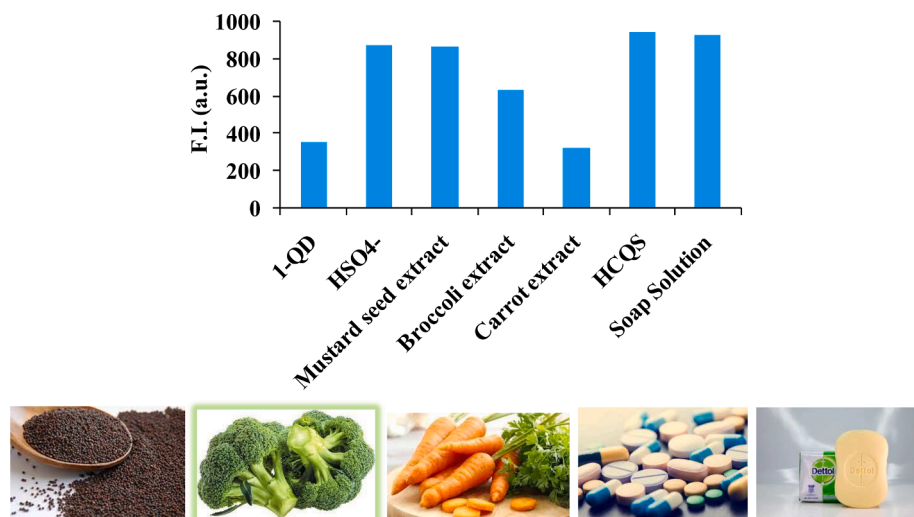

Fig. 5. Fluorescence titration experiments of *1-QDs* in CH$_3$CN:H$_2$O (2:1, v/v) (pH = 7, HEPES buffer) in the presence of various concentrations of sensed ions (a) Cu^{2+}, (b) Hg^{2+} and (c) HSO$_4^-$ excited at 350 nm. Inset: Plot of fluorescence intensity at 423 nm versus the concentration of added, Cu^{2+}, Hg^{2+} and HSO$_4^-$ ions.

Fig. 6. Bar graph showing the fluorescence changes upon addition of mustard seed extract, broccoli, carrot extract, medicine (HCQS), and soap in the aqueous solution of *1-QDs*.

addition of 100 μL of mustard seed extract and broccoli extract into the (2 mg/100 mL) solution of the *1-QDs* in CH₃CN:H₂O (2:1, v/v) (pH = 7, HEPES buffer) resulted in a three-fold and two-fold increase in fluorescence in comparison with that of *1-QDs* respectively (Fig. 6), which signifies the presence of HSO_4^- ion in the mustard seed extract and broccoli. On the contrary, the carrot extract resulted in negligible changes in the emission spectrum of *1-QDs*, pointing to absence of HSO_4^- ion in carrot extract.

The fluorescence emission spectrum was also recorded in the presence of medicine, hydroxychloroquinsulphate (HCQS) and soap solution. The medicine was taken in powdered form and 2 mg of it was dissolved in 10 mL of water. The emission spectrum observed a

significant enhancement with the addition of 20 μL medicinal solution to the *1-QDs*, pointing towards the recognition of HSO_4^- ion in the medicinal solution. Further, the soap solution (which generally contains sodium bisulfate and sodium laureth sulphate) was also tested and it also resulted in increased fluorescence intensity indicating the presence of HSO_4^- ion. Hereafter, it can be said that the *1-QDs* can be effectively applied for the detection of HSO_4^- in daily utility products (Fig. 6).

3.4. Plausible sensing model for *1-QDs*

In the presence of all the investigated anions, the light blue fluorescence of *1-QDs* remained intact and became dark blue only in the case
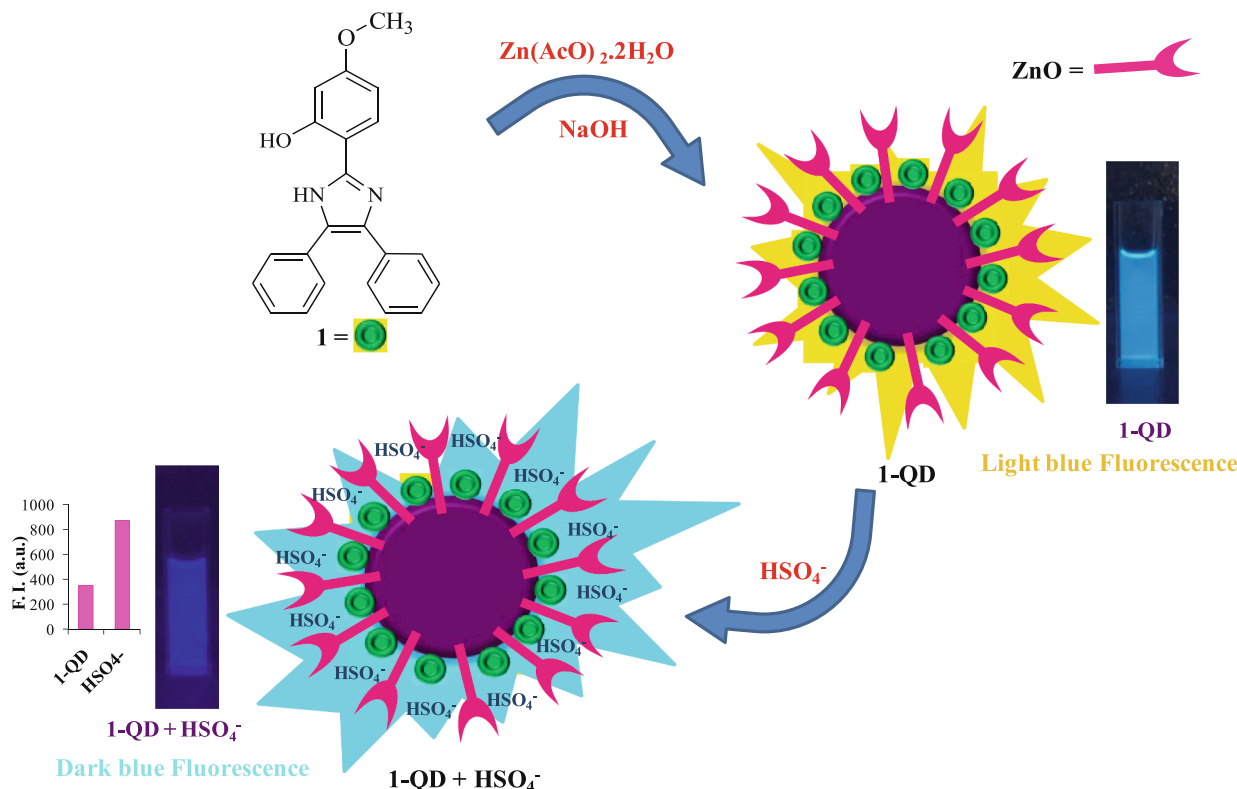
Scheme 2. Schematic representation of the probable mechanism and interactions between the quantum dots and the sensed anion, HSO_4^-.

of HSO$_4^-$ ion. Thus, the developed quantum dots provided the selective fluorescence colour changes as well as spectral changes for HSO$_4^-$ ions amongst other anions (Fig. S10).

The mechanism of fluorimetric sensing was described on the basis of modulation of energy charge transfer process and complexation of HSO$_4^-$ ions with the **1-QDs**. In the emission spectra, the fluorescence intensity peak of **1-QDs** displayed a remarkable blue shift along with enhancement upon the addition of the HSO$_4^-$ anion. This could be the outcome of complex formation between the functionalities of **1-QDs** and the recognized anion (Scheme 2). The functional groups (–OH, –NH and –OCH$_3$) present in **1** interacts with the ZnO present in **1-QDs**, which might have increased their acidity, making their binding with anionic species easier. Therefore, the sensed anion, HSO$_4^-$ form complex with these functionalities in **1-QDs**. These results lead to the creation of a new fluorescence switch-on sensor for HSO$_4^-$ ions in the water system.

3.5. Comparison of present work with literature sensors for HSO$_4^-$

Table 1 shows the comparison of the present quantum dots sensor, **1-QDs**, with some earlier reported receptors for HSO$_4^-$. There is presently no quantum dots sensor in literature based on benzimidazole till date for HSO$_4^-$ anion. The LOD value for HSO$_4^-$ anion is observed to be the lowest of all the compared sensors in the literature. It is clear from the table that most of the sensors detect HSO$_4^-$ anion by the hydrogen bond interactions with –NH of the imidazole ring. Whereas, in the present work, the acidic nature of functional groups present in **1** is enhanced due to the formation of ZnO quantum dots (**1-QDs**) which in turn interacts

with sensed ionic species and results in increased fluorescence. Furthermore, the **1-QDs** are utilized to recognize HSO$_4^-$ anion in real samples such as edible materials and medicines. Therefore, the quantum dots sensor **1-QDs** become better than others due to their simple and one-pot synthesis, low LOD values and real-life applications.

4. Conclusions

In summary, we have successfully synthesized water-stable fluorescent quantum dots, **1-QDs** possessing benzimidazole for detection of HSO$_4^-$ in CH$_3$CN:H$_2$O (2:1, v/v) (pH = 7, HEPES buffer). The addition of HSO$_4^-$ ions to the quantum dots, **1-QDs**, showed large fluorescence enhancement. This result was utilized for the real-time applicability of **1-QDs** in recognizing HSO$_4^-$ ion. The quantum dots were successfully used to determine HSO$_4^-$ ion in daily utility products such as medicine and soap solution. Also, they were found feasible to determine HSO$_4^-$ ion in edible materials like mustard seeds.
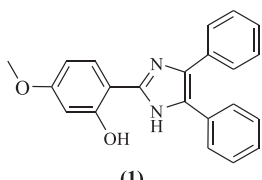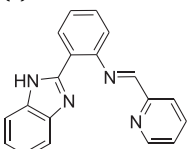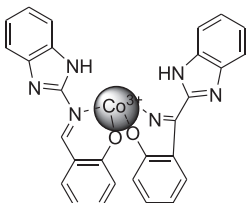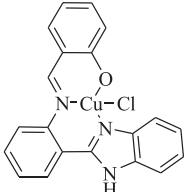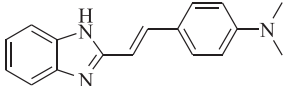
CRediT authorship contribution statement

Gitanjali Jindal: Methodology, Data curation, Formal analysis, Visualization, Writing – original draft. **Navneet Kaur:** Conceptualization, Writing – review & editing, Supervision, Project administration.

Declaration of Competing Interest

The authors declare that they have no known competing financial

Table 1
Comparison of the present work with previous literature reports.

S. No.	Sensor	Solvent system	Method for sensing	LOD (M)	Reference
1.	Quantum dots based on (1)	CH$_3$CN:H$_2$O (2:1, v/v)	Fluorescence	3.17×10^{-9}	[Present work]
2.		CH$_3$CN:H$_2$O (8:2, v/v)	Fluorescence	1.58×10^{-6}	[49]
3.		CH$_3$OH:H$_2$O (8:2, v/v)	UV–vis and electrochemical	63×10^{-6}	[50]
4.		H$_2$O:DMSO (9:1, v/v)	UV–vis, Fluorescence and electrochemical	3.18×10^{-7}	[51]
5.		CH$_3$OH	UV–vis	7.96×10^{-6}	[52]

interests or personal relationships that could have appeared to influence the work reported in this paper.

Acknowledgements

Appendix A. Supplementary data

Supplementary data to this article can be found online at https://doi.org/10.1016/j.jphotochem.2021.113652.

References

[1] J.L. Sessler, P.A. Gale, W.S. Cho, RSC (2006) 1–26.
[2] (a) T. Gunnlaugsson, M. Glynn, G.M. Tocci, P.E. Kruger, F.M. Pfeffer, Coord. Chem. Rev. 250 (2006) 3094–3117;
(b) R. Martinez-Manez, F. Sancenon, Chem. Rev. 103 (2003) 4419–4476.
[3] (a)(a) Z. Xu, X. Chen, H.N.J. Yoon, Chem. Soc. Rev. 39 (2010) 127–137; (b) V. Amendola, L. Fabbrizzi, Chem. Commun. (2009) 513–531.c) M. Cametti, K. Rissanen, Chem. Commun. (2009) 2809–2829.
[4] (a) C. Caltagirone, P.A. Gale, P.A. Gale, S.E. Garcia-Garrido, J. Garric, Chem. Soc. Rev. 38 (2009) 520–563;
(b) P. Prados, R. Quesada, Supramol. Chem. 20 (2008) 201–216;
(c) P.A. Gale, R. Quesada, Coord. Chem. Rev. 250 (2006) 3219–3244.
[5] G.W. Lee, N. Singh, H.J. Jung, D.O. Jang, Tetrahedron Lett. 50 (2009) 807–810.
[6] M.S. Kumar, S.L.A. Kumar, A. Sreekanth, Anal. Methods 5 (2013) 6401.
[7] X. Lou, D. Ou, Q. Li, Z. Li, Chem. Commun. 48 (2012) 8462–8477.
[8] H.J. Kim, S. Bhuniya, R.K. Mahajan, R. Puri, H. Liu, K.C. Ko, J.Y. Lee, J.S. Kim, Chem. Commun. (2009) 7128–7130.
[9] W. Lu, J. Zhou, K. Liu, D. Chen, L. Jiang, Z. Shen, J. Mater. Chem. B 1 (2013) 5014–5020.
[10] a) P. Ebbersen, J. Immunol. 109 (1972) 1296–1299;
b) T.J. Grahame, R.B. Schlesinger, Inhal. Toxicol. 17 (2005) 15–27;
c) D.P. Cormode, S.S. Murray, A.R. Cowly, P.D. Beer, Dalton. Trans. (2006) 5135–5140.
[11] a) J.J. He, F.A. Quiocho, Science 251 (1991) 1479–1481;
b) E.V. Anslyn, J. Smith, D.M. Kneeland, K. Ariga, F.Y. Chu, Supramol. Chem. 1 (1993) 201–208;
c) J.W. Pflugrath, F.A. Quiocho, Nature 314 (1985) 257–260.
[12] a) P.S. Shah, T. Balkhair, Environ. Int. 37 (2011) 498–516;
b) B.P. Leaderer, Science 218 (1982) 1113–1115.
[13] N. Fujioka, V. Fritz, P. Upadhyaya, F. Kassie, S.S. Hecht, Mol. Nutr. Food Res. 60 (2016) 1228–1238.
[14] A.S. Keck, J.W. Finley, Int. Can. Therapies 3 (2004) 5–12.
[15] M.G. Botti, M.G. Taylor, N.P. Botting, J. Biol. Chem. 35 (1995) 20530–20535.
[16] J. A. Marx, R. S. Hockberger and R. M. Walls, Rosen's Emergency Medicine: 8th edition (2014).
[17] Q. Li, Y. Guo, S. Shao, Analyst 137 (2012) 4497–4501.
[18] A.I. Ekimov, A.L. Efros, A.A. Onushchenko, Solid State Commun. 56 (1985) 921–924.
[19] L.E. Brus, J. Chem. Phys. 79 (1983) 5566–5571.
[20] A.I. Ekimov, A.A. Onushchenko, Sov. Phys. Semicond. 16 (1982) 775–778.
[21] D. Bera, L. Qian, T.-K. Tseng, P.H. Holloway, Materials 3 (2010) 2260–2345.
[22] C.Y. Chen, C.T. Cheng, C.W. Lai, P.W. Wu, K.C. Wu, P.T. Chou, Y.H. Chou, H. T. Chiu, Chem. Commun. (2006) 263–265.
[23] E.R. Goldman, I.L. Medintz, J.L. Whitely, A. Hayhurst, A.R. Clapp, H.T. Uyeda, J. R. Deschamps, M.E. Lassman, H. Mattoussi, J. Am. Chem. Soc. 127 (2005) 6744–6751.
[24] I.L. Medintz, A.R. Clapp, H. Mattoussi, E.R. Goldman, B. Fisher, J.M. Mauro, Nat. Mater. 2 (2003) 630–638.
[25] Y. Kim, J.B. Jeon, J.Y. Chang, J. Mater. Chem. 22 (2012) 24075–24080.
[26] G. Singh, A. Choudhary, D. Haranath, A.G. Joshi, N. Singh, S. Singh, R. Pasricha, Carbon 50 (2012) 385–394.
[27] N.R. Jana, H.-H. Yu, E.M. Ali, Y. Zheng, J.Y. Ying, Chem. Commun. (2007) 1406–1408.
[28] H. Sharma, A. Singh, N. Kaur, N. Singh, ACS Sustainable Chem. Eng. 1 (2013) 1600–1608.
[29] H. Sharma, N. Kaur, T. Pandiyan, N. Singh, Sens. Actuators B: Chem. 166–167 (2012) 467–472.
[30] N. Baig, I. Kammakakam, W. Falath, Mater. Adv. 2 (2021) 1821–1871.
[31] A.T. Wright, E.V. Anslyn, Chem. Soc. Rev. 35 (2006) 14–28.
[32] H.N. Kim, W.X. Ren, J.S. Kim, J. Yoon, Chem. Soc. Rev. 41 (2012) 3210–3244.
[33] S. Liu, J. Tian, L. Wang, Y. Zhang, X. Qin, Y. Luo, A.M. Asiri, A.O.A. Youbi, X. Sun, Adv. Mater. 24 (2012) 2037–2041.
[34] W. Lu, X. Qin, S. Liu, G. Chang, Y. Zhang, Y. Luo, A.M. Asiri, A.O.A. Youbi, X. Sun, Anal. Chem. 84 (2012) 5351–5357.
[35] W.I. Park, G.C. Yi, Adv. Mater. 16 (2004) 87–90.
[36] R. Könenkamp, R.C. Word, C. Schlegel, Appl. Phys. Lett. 85 (2004) 6004–6006.
[37] Z.K. Tang, G.K.L. Wong, P. Yu, M. Kawasaki, A. Ohtomo, H. Koinuma, Y. Segawa, Appl. Phys. Lett. 72 (1998) 3270–3272.
[38] T. Makino, C. Chia, Y. Segawa, M. Kawasaki, A. Ohtomo, K. Tamura, Y. Matsumoto, H. Koinuma, Appl. Surf. Sci. 189 (2002) 277–283.
[39] K.F. Lin, H.M. Cheng, H.C. Hsu, L.J. Lin, W.F. Hsieh, Chem. Phys. Lett. 409 (2005) 208–211.
[40] H. Zhou, H. Alves, D.M. Hofmann, W. Kriegseis, B.K. Meyer, Appl. Phys. Lett. 80 (2002) 210–212.
[41] Y.L. Wu, C.S. Lim, S. Fu, A.I.Y. Tok, H.M. Lau, F.Y.C. Boey, X.T. Zeng, Nanotechnology 18 (2007) 215604.
[42] R.L. Siqueira, I.V.P. Yoshida, L.C. Pardini, M.A. Schiavon, Mater. Res. 10 (2007) 147–151.
[43] A. Aboulaich, C.-M. Tilmaciu, C. Merlin, C. Mercier, H. Guilloteau, G. Medjahdi, R. Schneider, Nanotechnology 23 (2012) 335101.
[44] S. Yang, H. Kou, H. Wang, K. Cheng, J. Wang, New J. Chem. 34 (2010) 313–317.
[45] E. Oliveira, J.D. Nunes-Miranda, H.M. Santos, Inorg. Chim. Acta 380 (2012) 22–30.
[46] H.A. Benesi, J.H. Hildebrand, J. Am. Chem. Soc. 71 (1949) 2703–2707.
[47] G.L. Long, Anal. Chem. 55 (1983) 712A–724A.
[48] R.R. Nair, M. Raju, S. Bhai, I.H. Raval, S. Haldar, B. Ganguly, P.B. Chatterjee, Analyst 144 (2019) 5724–5737.
[49] P. Saluja, N. Kaur, N. Singh, D.O. Jang, Tetrahedron 68 (2012) 8551–8556.
[50] H. Sharma, V.K. Bhardwaj, N. Kaur, N. Singh, D.O. Jang, Tetrahedron Lett. 54 (2013) 5967–5970.
[51] B. Sen, M. Mukherjee, S. Pal, S. Sen, P. Chattopadhyay, RSC Adv. 5 (2015) 50532–50539.
[52] D. Phapale, A. Khushwaha, D. Das, Spectrochimica. Acta A Mol. Biomol. Spectrosc. 214 (2019) 111–118.